

Recognizing partial burn operation in an HCCI engine

Ahmad Ghazimirsaid¹, Mahdi Shahbakhti², Charles Robert Koch^{1*}

¹*Department of Mechanical Engineering, University of Alberta, Edmonton, AB T6G 2G8*

²*Department of Mechanical Engineering, KNT University of Technology, Tehran, Iran*

1. Abstract

Homogeneous Charge Compression Ignition (HCCI) has potential to improve the efficiency of Spark Ignition (SI) or Compression Ignition (CI) engines particularly at part load near the partial burn/misfire limit. Two challenges of HCCI combustion are: maintaining constant ignition timing despite no direct mechanism to start combustion, and to expand the part load region of HCCI near the misfire limit. To accomplish these goals it is critical to have accurate online and offline estimates of ignition timing.

For offline operating condition ignition timing calculation, a new method is proposed which combines the Coefficient of Variation of Indicated Mean Effective Pressure (COV_{imep}) and percentage of cycles with less than 90 percent heat release of previous cycle. Particularly near the partial burn/misfire limit, this method is more reliable than just COV_{imep}. For online ignition timing estimates, a new method in which the ratio of the peak of main stage and cool flame stage of heat release curve (HTR to HTRLTR Peak Ratio) is used for each cycle. Using this method, normal and partial burn engine cycles can be determined in realtime for fuels exhibiting a cool flame.

The two methods are tested on 115 HCCI experimental operating points, in which 300 cycles of cylinder pressure data are collected, and are found to be more reliable than existing methods in the literature. With a more reliable partial burn ignition timing criteria, this information could be used in future studies in a feedback control to stabilize ignition timing in these regions and thus extend the useful operating range of HCCI.

2. Introduction

HCCI combustion has potential for improved fuel economy, very low oxides of nitrogen (NO_x) and low particulate emissions. HCCI is considered as a high-efficiency alternative to spark-ignited (SI) gasoline operation and as a low-emissions alternative to traditional diesel compression ignition (CI) combustion. However, the practical application of HCCI requires overcoming several technical hurdles. HCCI misfire or partial-burn is undesirable because it results in increased exhaust emissions and reduces engine power output.

A partial burn or misfire event is a lack of combustion which results in a momentary lack of torque. Misfire or partial burn leads to an engine speed decrease [1] and is undesirable since it can lead to speed and torque fluctuations, increased exhaust emissions [2], and unburned fuel in the exhaust that will eventually damage the catalytic converter [3]. In particular, there is a high risk of partial burn or misfire in HCCI operation, which have a much more destructive consequence on the engine's performance and emission than SI combustion [4].

As the cylinder charge is made leaner (with excess air) or more dilute (with a higher burned gas fraction from residual gases or exhaust gas recycle) the cycle-by-cycle combustion variations increase until some partial burn cycles occur. Further leaning or more charge dilution results in reaching the misfire limit as a portion of the cycles fail to ignite. Such operation is undesirable from the point of efficiency, HC emissions, torque variations and roughness [5]. Retarding the combustion phasing allows higher loads before knock becomes prohibitive [6].

It is difficult to describe the dynamics of HCCI near the partial burn operating region and thus to control HCCI effectively to avoid misfires [7]. The understanding of the HCCI engine behavior in case of misfire and delayed combustion is an important first step to provide a control strategy to avoid partial burn and misfire and expand HCCI operation close to this region. Techniques for partial burn recognition, which are mainly based on the analysis of in-cylinder pressure, ionization current and crankshaft angular speed are detailed in [8]. Cost effective methods of partial burn detection use

*Corresponding author: bob.koch@ualberta.ca

existing crankshaft sensors and are based on crankshaft speed fluctuation [9, 10, 11, 12]. Here, equivalent methods to detect partial burn in terms of crank-angle based parameters and cylinder pressure are proposed.

In the next section of this paper, the single cylinder experimental setup used to collect the data is briefly described. Then, the procedure to find an offline partial burn operating condition in HCCI engine is outlined. The cyclic method for recognition of partial burn and normal operating is discussed in the next section. Finally, the effect of online method on location of ignition timing for all operating points is investigated in order to choose the proper parameters to be used as a feedback signal in future HCCI closed loop control.

3. Engine Setup

A single cylinder Ricardo Hydra Mark 3 block fitted with a VVT Mercedes E550 cylinder head is used [13] and is shown schematically in Figure 1. The engine with specifications given in Table 1 [14] is outfitted with a Kistler piezo electric pressure transducer. The intake air is heated with a temperature controlled 600W electric heater, while the intake pressure is adjusted with an externally driven supercharger. N-heptane and iso-octane are individually port injected to set octane values with two injectors driven by a dSpace-MicroAutobox ECU.

Cylinder pressure is recorded 3600 times per crank revolution, and then analyzed for the pertinent combustion metrics, such as CA10 and heat release. All other parameters are logged at 100 Hz using A&D Baseline DAC. The operating points span the range between normal operating condition to the misfire condition. All of the engine operating points are at steady-state operating conditions (inputs to engine and engine speed held constant). The tests operating conditions are listed in Table 2.

Table 1: Configuration of the Ricardo single-cylinder engine

Parameters	Values
Compression Ratio	12
Bore × stroke [mm]	97 × 88.9
Connecting Rod Length [mm]	159
Displacement [L]	0.653
Valve Lift [mm]	9.3
Valves	4

Table 2: Engine operating conditions

Parameter	Range
Manifold Temperature [°C]	85-97
Fuel Octane Number [PRF]	0,10,20,30,40
Manifold Pressure [kPa]	90-120
Equivalence Ratio [-]	0.29-0.55
External EGR [%]	0
Engine Speed [RPM]	1021-1074

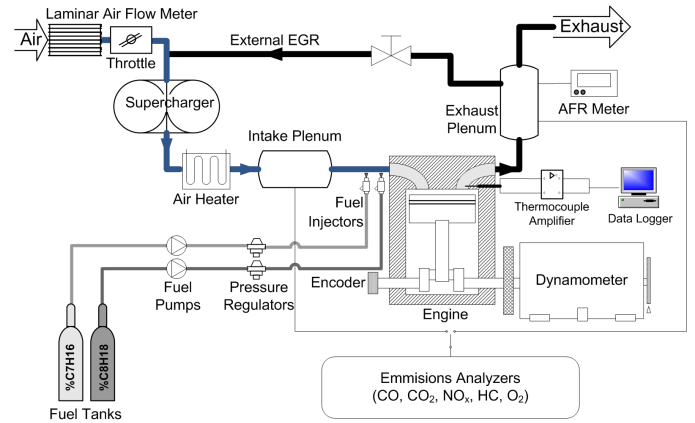


Figure 1: Schematic of the experimental setup

4. Results and Discussions

Offline method for partial burn region recognition

To recognize the misfire limit using a single parameter, several techniques using IMEP (Indicated Mean Effective Pressure) have been used [4, 15, 14]. In [15] a standard deviation of IMEP more than 2% is deemed unacceptable as this corresponds to the appearance of partial burn and misfire cycles. The coefficient of variation, is used to measure cyclic variability of engine parameters [16]. Applying the same criteria to our 115 operating points, it is found that COV_{imep} (Coefficient of variation of IMEP) is not a single reliable parameter in recognizing high cyclic variation since there exist several operating points having high COV_{imep} but have few or zero partial burn cycles. A P_{Burn} (partial burn) cycle is defined as when the total heat release is less than 90% of previous cycle. That is, a cycle with 10% reduction in total heat release compared to its previous cycle is considered as a partial burn cycle. An operating point is

considered partial burn operating point if it contains more than 14% partial burn cycles [17].

To confirm the above assumption, the average total heat release versus COV_{imep} for all the 115 operating points are shown in Figure 2. As it can be seen from Figure 2, there are several operating points with large COV_{imep} values ($0.05 < COV_{imep} < 0.15$) which have high total heat release and therefore do not belong to partial burn operating region. The few operating points with ($0.15 < COV_{imep}$) are very close to complete misfire and therefore are excluded from partial burn operating region category. Also it can be illustrated in Figure 2 (below the lower line) there is a minimum COV_{imep} and there exist no points with low total heat release and low COV_{imep} at the same time. On the other hand, above the higher line, no points with high total heat release and high COV_{imep} can be found in Figure 2.

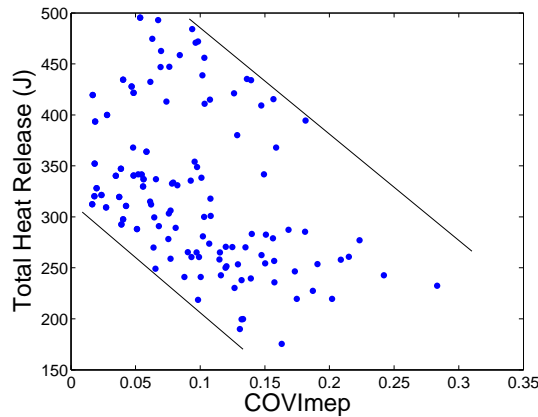


Figure 2: Total Heat Release versus COV_{imep}

The total heat release of all operating points are shown versus their number of partial burn cycles in Figure 3. The downward trend of heat release is visible for an increase in the number of partial burn cycles in the operating points. Most of the operating points to the right of dashed red line in Figure 3 ($0.14 < P_{BurnCycles}$) have their total heat release less than 300 J. However, there are two operating points in the circle with high total heat release in the above-defined region. Observing all the operating points, all the operating points with total heat release below than 300J, have been observed as operating points near partial burn condition. Furthermore, based on the earlier definition of partial burn criteria, all the operating points containing more than 14% partial burn cycles are considered in the partial burn region. If partial burn is defined as points having a total heat release less than 300J and more than 14% partial burn cycles then the two points in region II will not be identified correctly as partial burn operating points.

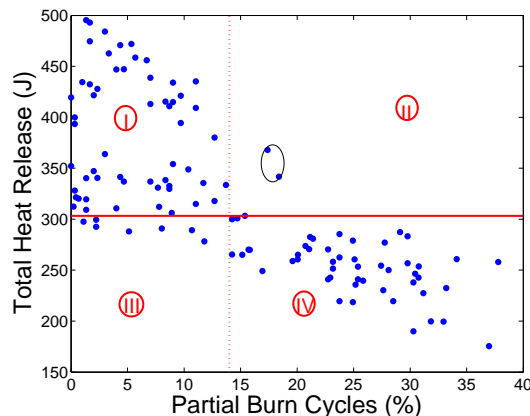


Figure 3: Total Heat Release versus Partial Burn Cycles

COV_{imep} versus percent of partial burn cycles for all 115 operating points is shown in Figure 4.

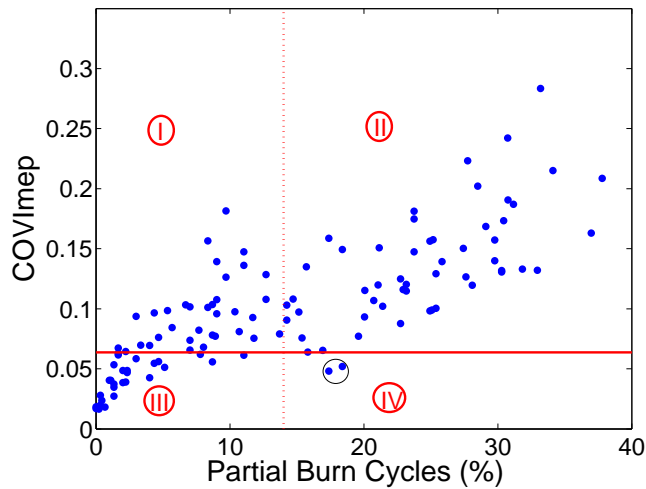


Figure 4: Percent of cycles with less than 90 percent of previous cycle versus COV_{imep}

Based on the definition of partial burn operating points having more than 14% partial burn cycles, then the partial burn operating points are specified as the points inside region II and IV in Figure 4. The two points in the circle in region IV are the same points in region II of Figure 3 which work in normal operating condition. Figure 4 show that the two points in the circle have their COV_{imep} less than 6%. Therefore all the operating points with COV_{imep} higher than 6% and more than 14% partial burn cycles are considered as the partial burn operating points with no error.

Online method for partial burn region recognition

A new criteria, called HTR to HTRLTR ratio, is defined for online recognition of operating mode. This is defined as: $R_{HLLTR} = \frac{HTR_{max}}{HTR_{max} + LTR_{max}}$ the ratio of peak of main stage to total of peak of main stage and cool flame stage of heat release curve. $R_{HLLTR} = 10.70$ for the sample points N with low cyclic variations and conditions 1025 RPM, $T_{runner} 81\text{ }^{\circ}\text{C}$, $P_{man} 115\text{ kPa}$, ON 30, $\lambda 2.28$, Total HR 420 J, $COV_{imep} 1.7\%$ and P_{Burn} cycles 0% representing a normal operating condition and Point P with high cyclic variations and conditions $R_{HLLTR} = 2.26$, 1025 RPM, $T_{runner} 80\text{ }^{\circ}\text{C}$, $P_{man} 95\text{ kPa}$, ON 0, $\lambda 2.61$, Total HR 232 J, $COV_{imep} 28\%$ and P_{Burn} cycles 33% representing a partial burn operating condition is shown in Figure 5 along with point N.

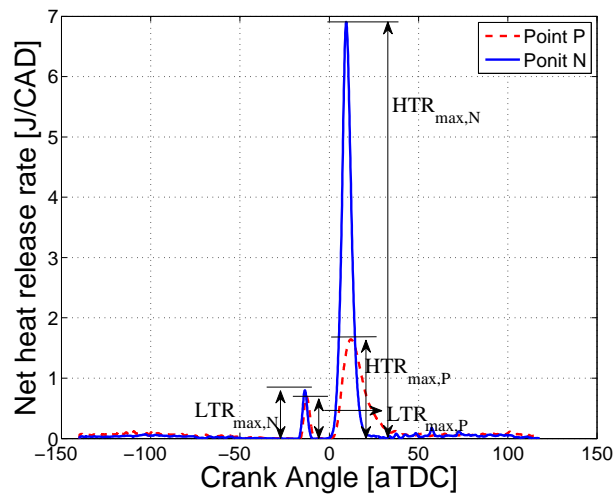


Figure 5: HTR to HTRLTR peak definition for two sample points N and P of Figure 4

The relation between R_{HLLTR} and the location of CA10 (crank angle where 10 percent of total heat release of combustion

has occurred) for point P, is shown in Figure 6 [18]. The taller (blue) bars correspond to the R_{HLTR} where CA10 occur on the main stage while the shorter (red) bars correspond to the cool flame stage of combustion. Figure 6 shows that for $R_{HLTR} > 0.73$, CA10 always occur on the main stage of combustion.

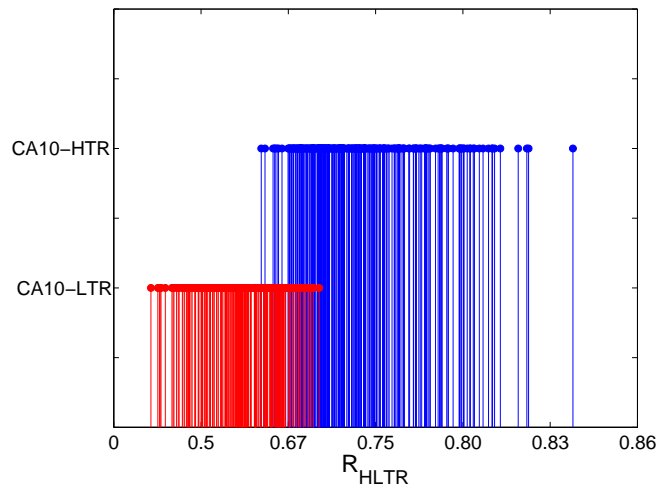


Figure 6: Effect of HTR to HTRLTR peak ratio on location of CA10 for point P

Online method for all operating points

The percentage of cycles with $R_{HLTR} < X$ for each operating point, representing the cycles with their CA10 occurred on LTR (Low Temperature Region), versus percent of partial burn cycles for that operating point is shown in Figure 7. As expected, the value of X changes depending on the octane number and is shown for different octane number values in Figure 7. The vertical line at 14% in Figure 7 represents the line above which we define a partial burn operating point. The diagonal dotted line indicates a perfect partial burn prediction using R_{HLTR} . For most of the operating points with high percent of partial burn cycles, the percent of cycles with $R_{HLTR} < X$ increase which corresponds to the cycles where the CA10 occur on LTR. This means that for those cycles with $R_{HLTR} < X$ not all the CA10 fall near main stage of combustion which could be problematic since it then does not reflect the start of combustion of the main stage anymore. The closer the percentage of bulk of CA10 gets to the main stage of combustion the higher ratio of R_{HLTR} will be. This shows that as the ratio of R_{HLTR} decrease, tendency of calculated CA10 to move towards the early stage of combustion increases. Also, Figure 7 shows that partial burn cycles can be predicted online utilizing the percent of cycles with $R_{HLTR} < X$, where X is a tuned threshold for each octane number.

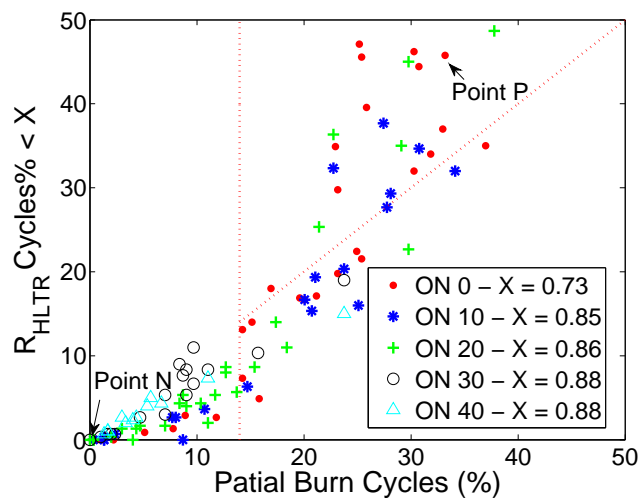


Figure 7: HTR to HTRLTR ratio lower than predetermined value versus partial burn cycles for all the data points

6. Conclusions

First, experimental data from HCCI engine collected at 115 operating points is used to define two criteria for partial burn operation, one used as offline criteria after collecting all the cycles and one online method by comparing the cyclic peak of main and cool flame stage of heat release curve. The criteria for characterizing HCCI engine operation as partial burn, when 14 percent of cycles are partial burn cycles is used. Finally, a new online partial burn criteria R_{HLTR} is defined and is found to achieve a rough correlation with the number of partial burn cycles when the threshold is adjusted for each octane number.

Acknowledgments AUTO21 Network of Centres of Excellence, the Canadian Foundation for Innovation (CFI) and the Natural Sciences and Engineering Research Council of Canada (NSERC) are gratefully acknowledged.

References

- [1] F. Ponti. Developmnet of a Torsional Behavior Powertrain Model for Multiple Misfire Detection. *Journal of Engineering for Gas Turbines and Power*, 130, 2008.
- [2] Z. Wu and A. Lee. Misfire Detection Using a Dynamic Neural Network with Output Feedback. *SAE Paper No. 980515*, 1998.
- [3] D. Moro, P. Azzoni, and G. Minelly. Misfire pattern recognition in high-performance SI 12-cylinder engine. *SAE Paper No. 980521*, 1998.
- [4] H. Zhao. *HCCI and CAI engines for the automotive industry*. Woodhead Publishing Limited, 2007.
- [5] J.B. Heywood. *Internal Combustion Engine Fundamentals*. McGraw HILL, 1988.
- [6] J-O Olsson, P. Tunestal, B. Johansson, S. Fiveland, J.R. Agama, and D.N. Assanis. Compression Ratio Influence on Maximum Load of a Natural Gas- Fueled HCCI Engine. *SAE Paper No. 2002-01-0111*, 2002.
- [7] K. L. Knierim, S. Park, J. Ahmed, and A. Kojic. Simulation of Misfire and Strategies for Misfire Recovery of Gasoline HCCI. *American Control Conference*, 2008.
- [8] F.L. Bue, A.D. Stefano, C. Giaconia, and E. Pipitone. Misfire Detection System based on the Measure of Crankshaft Angular Velocity. *Proceeding of the 11th annual AMAA conference, Berlin*, 2007.
- [9] P. Azzoni, D. Moro, C.M. Porceddu-Cilione, and G. Rizzoni. Misfire detection in a high-performance engine by the principal component analysis approach. *SAE Paper No. 960622*, 1996.
- [10] W. Ribbens and J. Park. Road Tests of a Misfire Detection System. *SAE Paper No. 940975.*, 1994.
- [11] J. Williams. An Overview of Misfiring Cylinder Engine Diagnostic Techniques Based on Crankshaft Angular Velocity Measurements. *SAE Paper No. 960039*, 1996.
- [12] A. Alkhateeb. *Robust Algorithms for Engine Misfire Detection*. PhD thesis, Oakland University, 2004.
- [13] R. Lupul. Steady State and Transient Characterization of a HCCI Engine with Varying Octane Fuel. Master's thesis, University of Alberta, 2008.
- [14] A.D. Audet. Closed Loop Control of HCCI using Camshaft Phasing and Dual Fuels. Master's thesis, University of Alberta, 2008.
- [15] M. Sjoberg and J. E. Dec. Comparing late-cycle autoignition stability for single- and two-stage ignition fuels in HCCI engines. *Proceeding of Combustion Institue*, 31:2895–2902, 2007.
- [16] M. Shahbakhti and C.R. Koch. Characterizing the cyclic variability of ignition timing in a homogenous charge compression ignition engine fueled with n-heptane/iso-octane blend fuels. *International Journal of Engine Research*, 9:361 – 397, 2008.
- [17] S.A. Ghazimirsaid, M. Shahbakhti, and C. R. Koch. Partial-burn crankangle limit criteria comparison on an experimental HCCI engine. *Proceeding of Combustion Institue - Canadian Section Spring Technical Meeting, University of Montreal, Quebec*, May 11-13, 2009.
- [18] A. Ghazimirsaid, M. Shahbakhti, and C.R. Koch. Comparison of Crankangle Based Ignititon Timing Methods on an HCCI Engine. *Submitted to the Proceeding of the ASME Internal Combustion Engine Division 2010 Fall Conference, San Antonio, USA.*, 2010.